Chemical Science

ROYAL SOCIETY OF CHEMISTRY

EDGE ARTICLE

View Article Online
View Journal | View Issue

Cite this: *Chem. Sci.*, 2025, **16**, 18775

All publication charges for this article have been paid for by the Royal Society of Chemistry

Received 13th August 2025
Accepted 9th September 2025

DOI: 10.1039/d5sc06158j

rsc.li/chemical-science

Büchner-type ring expansion of aromatic main-group biradicaloids toward phosphorus radical-derived NIR-II photothermal materials

Shihua Liu,[ab] Shunlin Zheng,[a] Jieli Lin,[a] Hansjörg Grützmacher,[a] Cheng-Yong Su[a] and Zhongshu Li*[a]

The Büchner reaction enables the construction of functionalized cycloheptatrienes and aromatic tropylium cations, and has recently been extended to the ring expansion of arenes with low-valent main-group systems. Although stable 6π-aromatic biradicaloids typically exhibit characteristic biradical reactivity, we leverage the aromaticity of dicarbondiphosphides (**1**) to achieve an unprecedented Büchner-type ring expansion, yielding air-stable aromatic 1,3-diphospholium cations (**3**). Multimodal characterization (NMR, UV-vis, SC-XRD, computational studies) confirms the 6π-aromaticity of **3**. Reduction of **3** yields stable 7π-electron neutral radicals (**4**), which contrast with conventional five-membered neutral radicals possessing 5π-electron systems. These radicals (**4a**: λ_{max} = 1113.2 nm; **4b**: λ_{max} = 1330.7 nm) exhibit strong second near-infrared biowindow (NIR-II, 1000–1350 nm) absorptions, and shown promising application potential as the first phosphorus radical-derived organic NIR-II photothermal materials.

Introduction

The Büchner reaction[1] has evolved into a versatile synthetic strategy for the direct construction of functionalized cycloheptatrienes[2] and aromatic tropylium cations from arenes.[3] Extensive mechanistic studies have established that this transformation proceeds through key norcaradiene intermediates (**A**, Fig. 1A) *via* a [2 + 1] cycloaddition between arenes and carbenes.[4] This mechanistic framework has been substantiated by the successful isolation of various norcaradiene derivatives (**A_I**, Fig. 1B).[5] Recent advances have demonstrated the adaptation of this ring-expansion reaction to main group element analogues of carbenes, including silylenes,[6] phosphinidenes,[7] and alumylenes.[8] The structural characterization of silicon- and phosphorus-containing norcaradiene analogues, specifically silanorcaradiene (**A_II**)[6a,9] and phosphanorcaradiene (**A_III**, Fig. 1B),[10] provides strong experimental validation of this mechanistic pathway.

Biradicaloids, defined as species comprising two covalently linked groups each carrying an unpaired electron that may combine to give a singlet ground state, have garnered significant interest due to their unique electronic configuration, unconventional reactivity profiles, and promising applications in materials science.[11] Despite their prevalence as transient intermediates in chemical processes,[12] molecular design principles such as steric

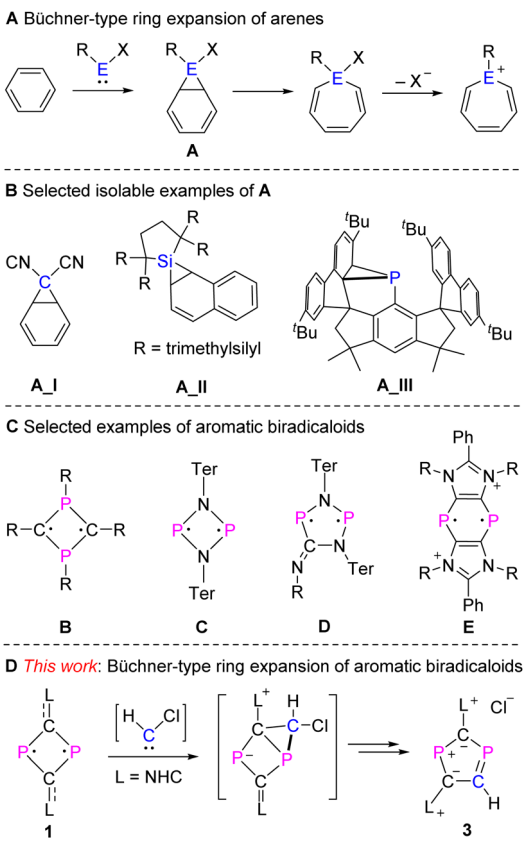

Fig. 1 (A) Büchner ring expansion of arenes; (B) selected isolable examples of **A**; (C) Selected examples of biradicaloids with considerable aromaticity; (D) the highlights of this work.

[a]*LIFM, IGCME, School of Chemistry, Sun Yat-Sen University, Guangzhou 510006, China. E-mail: lizhsh6@mail.sysu.edu.cn*

[b]*Key Laboratory of Guangdong Higher Education Institutions of Northeast Guangdong New Functional Materials, School of Chemistry and Environment, Jiaying University, Meizhou, 514015, Guangdong, China*

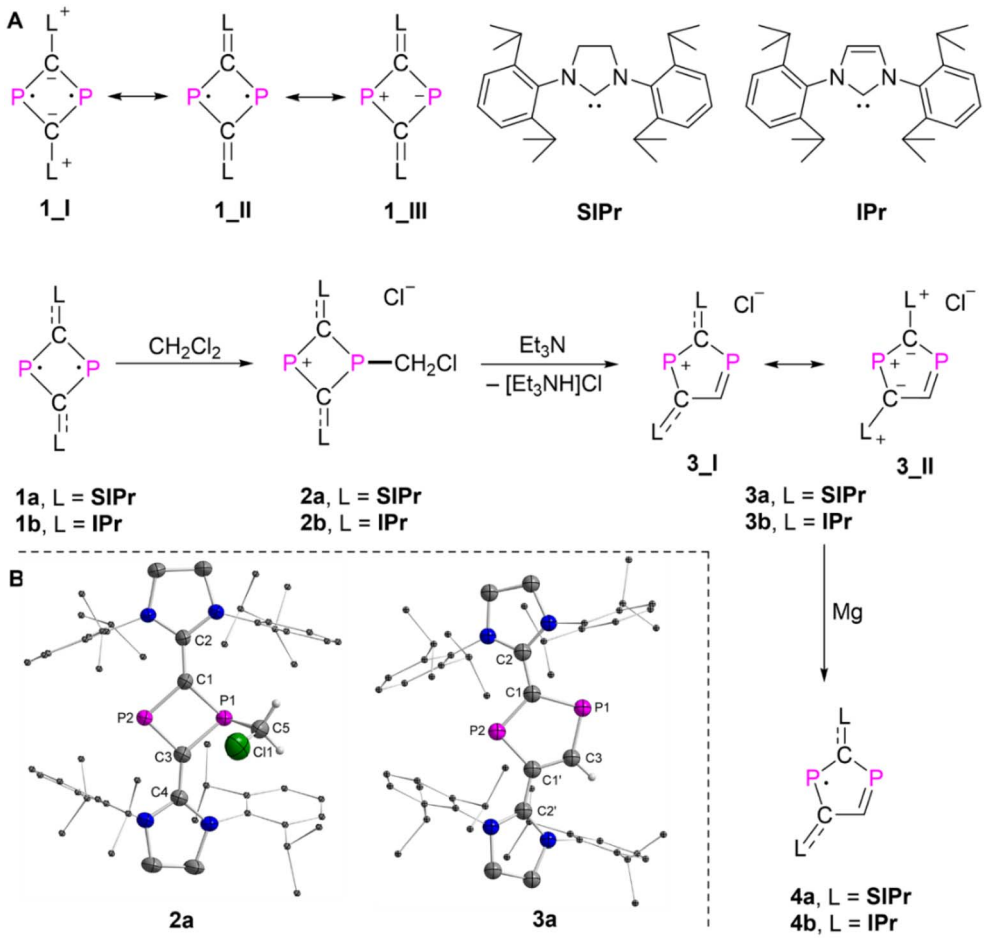

Fig. 2 (A) Synthesis of **2a**,**b**–**4a**,**b**; (B) Solid-state structure of **2a** and **3a** (ellipsoids are set to 50% probability; H atoms except H5A, H5B from **2a** and H3 from **3a**, solvents, and anions are omitted for clarity). Selected distances (Å): **2a**: P1–C1 1.816(2), P1–C3 1.809(2), P1–C5 1.836(3), P2–C1 1.755(2), P2–C3 1.735(2), C1–C2 1.407(3), C3–C4 1.407(3), C5–Cl1 1.784(3); 3a: P1–C1 1.7842(19), P1–C3 1.738(5), P2–C1 1.7546(17), C1′-C3 1.391, C1–C2 1.447(2), ′(1 + X, +Y, 1/2 − Z).

protection and spin delocalization have enabled the isolation of stable singlet biradicaloids – especially those exhibiting pronounced 6π-aromatic character.[13] Representative examples span diverse ring systems, including four-membered (**B**, and **C**),[14] five-membered (**D**),[15] and six-membered heterocycles (**E**, Fig. 1C).[16] Systematic investigations revealed that their chemical behaviour is governed by the inherent biradical character of their transannular radical centers, manifested in distinctive activation modes toward dihydrogen (H_2), disulphide, and unsaturated small molecules.[13d,17]

Motivated by the aromatic nature of these biradicaloids, we hypothesized that dicarbondiphosphides **1** (ref. 18) might exhibit reactivity patterns reminiscent of conventional aromatic compounds. Consistent with this premise, we previously demonstrated their utility as 6π-electron ligands in half-sandwich complexes formation.[19] Building on this foundation, Coburger and co-workers recently disclosed 6π-complexes of **1** with main-group metal cations[20] and a related five-membered diphosphaindeylide-based half-sandwich complex.[21] However, investigations into aromaticity-driven transformation in biradicaloids remains limited. In this context, we herein disclose a formal Büchner-type ring expansion of dicarbondiphosphides **1** to air-stable aromatic 1,3-diphospholium cations[22] **3** featuring two N-heterocyclic carbene (NHC)[23] substituents (Fig. 1C). Multimodal characterization, including multinuclear NMR spectroscopy, UV-vis absorption spectroscopy, single-crystal X-ray diffraction (SC-XRD), and computational studies, unequivocally confirm the structural and electronic features of **3**. Chemical reduction of **3** yields novel stable 7π-electron neutral radicals **4** (Fig. 2), whereas conventional five-membered cyclic neutral radicals predominantly possess a 5π-electron system.[24] These radicals (**4a**: λ_{max} = 1113.2 nm; **4b**: λ_{max} = 1330.7 nm) exhibit strong absorption in the second near-infrared region (NIR-II biowindow, 1000–1350 nm).[25] The temperature of **4a** and **4b** as a powders in NMR tube, increased to 63 °C and 56 °C in 180 s upon the irradiation of NIR-II laser (1064 nm, 0.5 W cm^{-2}), establishing it at the first phosphorus radical-based organic NIR-II photothermal material.[26]

Results and discussion

Synthesis and characterization of 1,3-diphospholium salts 3a,b

The electronic ground state of NHC substituted dicarbondiphosphides ($L_2C_2P_2$) can be described by three major

resonance forms: aromatic (1_I), biradicalloid (1_II), and zwitterionic (1_III, Fig. 2A), determining their unique reactivity in coordination chemistry and small molecule activation.[17e–g,19b,c,27] Treatment of **1a** (L = **SIPr** = 1,3-bis-(2,6-diisopropylphenyl) imidazolidin-2-ylidine) and **1b** (L = **IPr** = 1,3-bis-(2,6-diisopropylphenyl)imidazole-2-ylidine) with excess dichloromethane at room temperature (RT) afforded red powders **2a** ([(**SIPr**)$_2$C$_2$PP(CH$_2$Cl)]Cl) or **2b** ([(**IPr**)$_2$C$_2$PP(CH$_2$Cl)]Cl) in over 75% isolated yield (Fig. 2A). The ^{31}P NMR spectra of **2a** or **2b** displayed resonances at $\delta(^{31}P) = 452.9$ ppm (d, $^2J_{PP} = 65.2$ Hz) and 59.7 ppm (dt, $^2J_{PP} = 65.2$ Hz, $^2J_{PH} = 10.9$ Hz), or $\delta(^{31}P) = 396.0$ ppm (d, $^2J_{PP} = 67.7$ Hz) and 58.0 ppm (dt, $^2J_{PP} = 67.7$ Hz, $^2J_{PH} = 11.1$ Hz), respectively. The molecular structures of **2a,b** are confirmed by SC-XRD analyses (Fig. 2B and S22). In the case of **2a**, P1 adopts a trigonal pyramidal geometry ($\angle$CPC = 294.1°) with the formation of a new P1–C5 single bond (1.836(3) Å), while P2 is two-coordinated. The P1–C1 (1.816(2) Å) and P1–C3 (1.809(2) Å) are longer than P2–C1 (1.755(2) Å) and P2–C3 (1.735(2) Å). The NHC–C linkages (avg. 1.407 Å) show significant elongation compared to precursor **1a** (avg. 1.388 Å).[18a] These features correlate with positive charge delocalization across P2 and two NHC substituents.[27,28]

Deprotonation of **2a,b** with excess of triethylamine in acetonitrile at elevated temperature yielded yellow or pink powders **3a** ([(**SIPr**)$_2$C$_2$P$_2$(CH)]Cl) or **3b** ([(**IPr**)$_2$C$_2$P$_2$(CH)]Cl) in over 86% yield (Fig. 2A). Multinuclear NMR spectra and SC-XRD analyses confirmed the molecular structures of **3a,b** as cationic five-membered heterocycles with chloride as counterion. The ^{31}P NMR spectra of **3a** or **3b** exhibited resonances at $\delta(^{31}P) = 252.3$ ppm (d, $^2J_{PP} = 15.9$ Hz) and 216.9 ppm (dd, $^2J_{PP} = 15.9$ Hz, $^2J_{PH} = 45.3$ Hz), or $\delta(^{31}P) = 229.1$ ppm (d, $^2J_{PP} = 14.3$ Hz) and 207.9 ppm (dd, $^2J_{PP} = 14.3$ Hz, $^2J_{PH} = 45.3$ Hz), respectively. Those chemical shifts are comparable to the ones of precursors **1a** ($\delta^{31}P = 227.8$ ppm) and **1b** ($\delta^{31}P = 196.3$ ppm), which implies the presence of π-electron delocalization over two-coordinated phosphorus centers. An unambiguous assignment of the molecular structure of **3a** was obtained based on SC-XRD analyses (Fig. 2B). The central C$_3$P$_2$ ring is planar and the bond distances are in the range for delocalized P=C (1.78–1.74 Å) and C=C bonds (1.39 Å) [Σr_{cov}(P–C) = 1.86 Å, Σr_{cov}(P=C) = 1.69 Å, Σr_{cov}(C–C) = 1.50 Å, Σr_{cov}(C=C) = 1.34 Å].[29] The C–C bond lengths between the C$_3$P$_2$ ring and **SIPr** groups are 1.447(2) Å, much longer than typical C=C double bonds, indicating high electron donation from the **SIPr** groups to the central C$_3$P$_2$ ring. These structural features of **3** support the presence of an aromatic C$_3$P$_2$ ring (3_II). Indeed, this may be one reason why **3** is air stable. There are few low-valent organophosphorus compounds, which exhibit such high air stability.[30]

Computational insights into the electronic structure and a possible reaction mechanism

For a better understanding of the electronic structure of **3**, density functional theory (DFT) calculations[31] at the BP86/Def2SVP level were carried out for the simplified model **3a^M**,[18a] where the NHC **SIPr** were replaced with **SIMe** (**SIMe** = 1,3-dimethyl-imidazoline-2-ylidine). Detailed molecular orbital analysis (Fig. 3A) revealed that the highest occupied molecular orbital (HOMO), HOMO − 1, and HOMO − 6 predominantly comprise π-type orbitals of the C$_3$P$_2$ ring, while the lowest unoccupied molecular orbital (LUMO) primarily delocalizes across the phosphorus p-type orbital and the NHC-linked C=C π-type orbitals. Quantitative aromaticity assessment *via* the calculation of the nuclear independent chemical shift (BP86/Def2TZVP) yielded NICS(1) = −9.0 ppm for **3a^M** *versus* NICS(1) = −9.8 ppm for benzene, confirming significant aromatic character. This is in stark contrast to the weakly aromatic precursor **1a^M** (NICS(1) = −4.1 ppm). Intrinsic bond orbital (IBO)[32] analysis at PBE/Def2SVP level of theory further corroborate the electronic delocalization of the p-electron system (Fig. 3B). IBO-1 is mainly the π-type orbital of P=C bond, and IBO-2 or IBO-3 represent two π-type orbitals over the P–C–C or P–C units of the C$_3$P$_2$ ring that are polarized towards the NHC groups. These computational findings conclusively demonstrate a 6π-aromatic C$_3$P$_2$ core with positive charge delocalization over one of the phosphorus atoms and its two adjacent NHC groups in **3**.

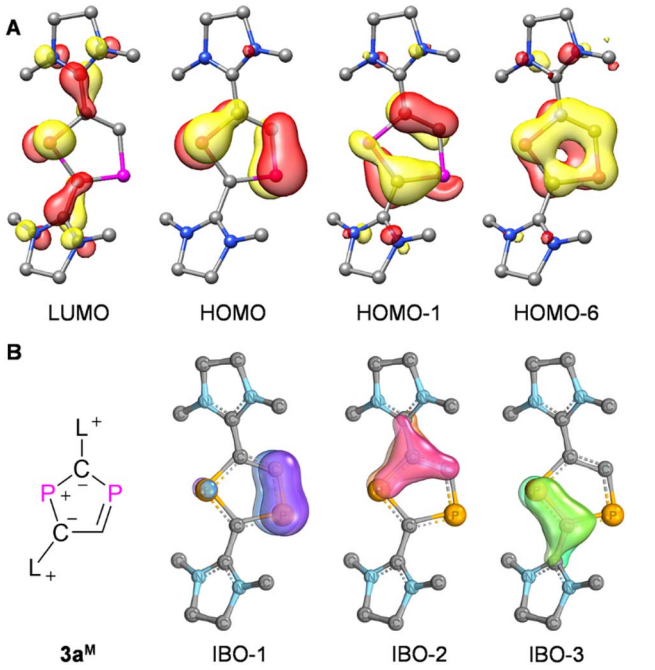

Fig. 3 (A) Kohn–Sham MOs (isovalue = 0.05) of simplified model **3a^M**; (B) Visual representation of selected IBOs. L = **SIMe**.

The mechanism leading to **3a** from the postulated intermediate formed by the deprotonation of **2a** was probed by DFT calculations at the SMD-BP86/Def2TZVP//BP86/Def2SVP level of theory for the model **3a^M**.[33] The minimum energy reaction pathway (MERP) for a possible rearrangement is shown in Fig. 4. The formation of a norcaradiene-type intermediate **IN2** (1.7 kcal mol^{-1}; *c.f* **A** In Fig. 1A) *via* [2 + 1] cycloaddition between one of the P–C bond and transient carbene is nearly thermal neutral and proceeds *via* the activated complex **TS1** (24.3 kcal mol^{-1}). The following P–C cleavage is easily achieved

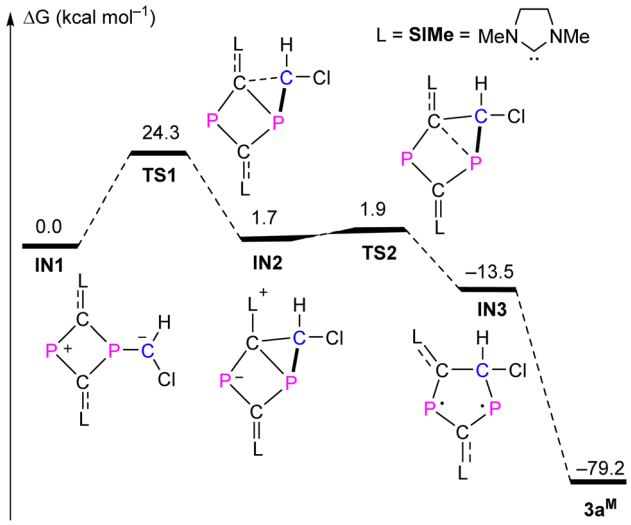

Fig. 4 MERPs for the formation of **3a**^{M}.

via **TS2** (0.2 kcal mol^{-1}) to generate ring-expanded **IN3** (−13.5 kcal mol^{-1}) in an exergonic reaction, which precludes any experimental detection of **IN2**. In the final step, C–Cl cleavage leads to the thermodynamically favored product **3a**^{M} (−65.7 kcal mol^{-1}). In addition, Schulz and co-workers have predicted that the ring-expansions of a four-membered diphosphadiazanediyl (**C**, Fig. 1C) with carbon monoxide (TS > 37 kcal mol^{-1})[15c] or isonitriles (TS > 48 kcal mol^{-1})[15a,34] to five-membered biradicaloids *via* biradical-type ring expansion mechanism are kinetically unfavourable. Thus, the formation of **3** likely proceeds *via* a Büchner-type mechanism *via* kinetically accessible transition states (<25 kcal mol^{-1}) with strong overall thermodynamic driving forces (>70 kcal mol^{-1}).

Synthesis and characterization of neutral 7π-electron radicals 4a,b

The cyclic voltammograms of a dichloromethane solution using 0.1 M [Bu$_4$N][PF$_6$] as the electrolyte show a reversible one-electron redox wave at $E_{1/2}$ = −1.61 V (**3a**, Fig. 5A) or −1.57 V (**3b**, Fig. S23) at a scan rate of 0.1 V s^{-1} (*vs.* Fc^{+}/Fc, Fc^{+} = ferrocenium, Fc = ferrocene), alluding to the generation of long-lived radicals. Chemically, **3a,b** can be quantitatively reduced with magnesium powder yielding highly air-sensitive neutral radicals **4a,b** as brown powders. The X-band CW-EPR spectra of **4a,b** (Fig. 5, and S23) in 2-methyltetrahydrofuran at RT show a doublet due to large isotropic ^{31}P hyperfine coupling constants (HFC) (av. g_{iso} = 2.0045, a_{iso}(P2) = 153.4 MHz for **4a**, g_{iso} = 2.0041, a_{iso}(P2) = 127.2 MHz for **4b**). In frozen solution at 100 K, the main features of the spectra of **4a,b** correspond to primarily anisotropic ^{31}P hyperfine interactions. The simulation of these spectra yielded the principal *g* values and HFCs for **4a** as *g* = [2.0027, 2.0090, 2.0020], and A(P2) = [5.1, 5.1, 450.2] MHz; for **4b** as *g* = [2.0031, 2.0072, 2.0020], and A(P2) = [3.2, 3.2, 375.1] MHz, respectively. An analysis of the solution and

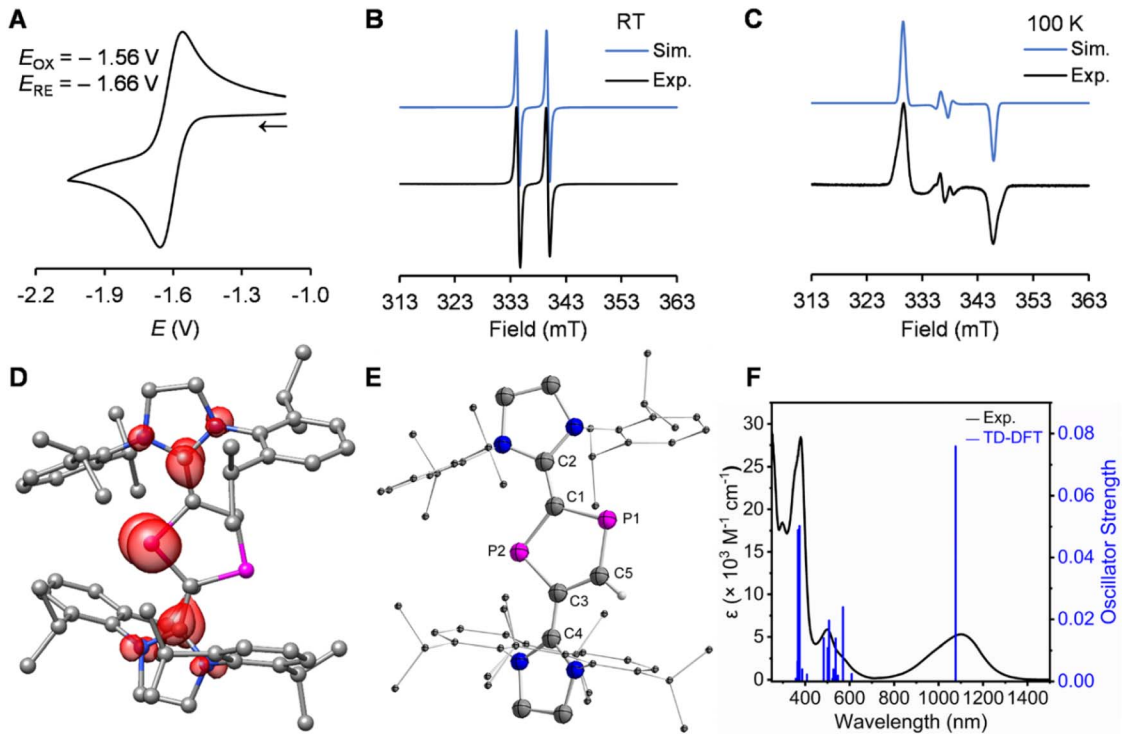

Fig. 5 (A) Cyclic voltammogram of **3a**; CW-EPR spectra at RT (B) and 100 K (C), calculated spin densities (density = 0.004) (D), solid-state structure (Ellipsoids are set to 50% probability; H atoms are omitted for clarity) (E), selected distances (Å): P1–C1 1.787(8), P1–C5 1.719(3), C5–C3 1.444(16), P2–C3 1.790(7), P2–C1 1.793(7), C1–C2 1.396(10), C3–C4 1.394(9), and experimental UV-Vis spectrum shown in black line and calculated Gaussian absorption bands shown in blue bars (F) of **4a**.

anisotropic solid-state EPR spectra allow to estimate the total spin density at P2 to be 41.6% for **4a** and 33.8% for **4b**, respectively. Consistent with these experimental data, DFT calculations at the BP86/Def2SVP level of theory on the optimized structures (see ESI for details) show that the Mulliken spin density (Fig. 5D) is primarily localized on P2 (43.5%), C2 (20.6%), and C4 (18.4%) for **4a**, and localized on P2 (38.3%), C2 (12.4%), and C4 (16.2%) for **4b**, respectively.

Brown single crystals of **4a** were grown from a saturated hexane solution *via* slow evaporation at RT and studied by SC-XRD analysis (Fig. 5E). Like in the precursor **3a**, the central C_3P_2 ring of **4a** is planar indicating significant electron delocalization over the ring skeleton. The P1 = C5 bond [1.719(3) Å *vs.* 1.738(5) in **3a**] is shortened while all other P–C bonds (avg. 1.79 Å) and C–C bonds (1.444(16) Å) are elongated as compared to those in **3a** indicating reduced aromaticity, but these bonds distances remain in the range of delocalized bonds.[29] The C=C bonds (avg. 1.40 Å) between the C_3P_2 ring and **SIPr** groups in **4a** are shorter than that in **3a** [1.447(2) Å] implying enhanced electron back-donating from the C_3P_2 ring to **SIPr**. The ultraviolet-visible (UV-Vis) absorption spectra of solutions of **4a,b** in toluene exhibit strong absorptions at λ_{max} = 1113.2 nm (**4a**) and 1330.7 nm (**4b**). According to time-dependent density functional theory (TD-DFT) calculations, these absorptions arise mainly from electronic transitions of the highest singly occupied molecular orbital (SOMO) to the singly unoccupied molecular orbital (SUMO) (π–π*), 1076.3 nm (**4a**, Fig. 5F), 1205.6 nm (**4b**, Fig. S27).

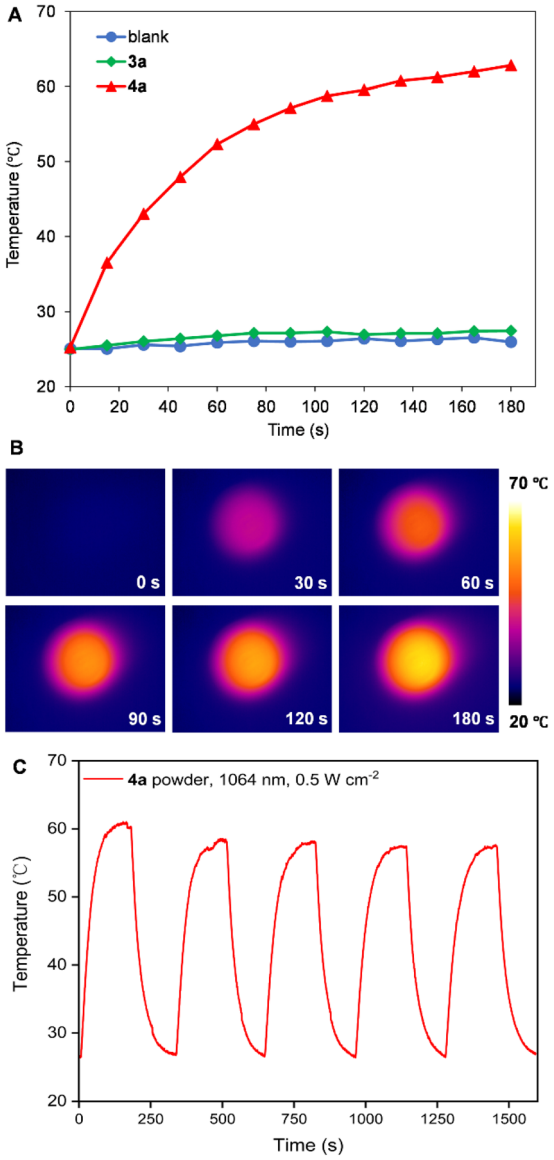

Fig. 6 (A) The temperature changes of blank, **3a** and **4a** powders under laser irradiation (1064 nm, 0.5 W cm^{-2}); (B) IR thermal images of **4a** powder; (C) Anti-photobleaching properties of **4a** powder during five cycles of heating–cooling processes.

Photothermal materials operating in NIR-II biowindow (1000–1350 nm)[25] have attracted significant interest due to advantages like deep tissue penetration and high maximum permissible exposure.[35] Nevertheless, designing organic NIR-II photothermal materials remains challenging.[35,36] Organic radicals are promising candidates, as their SOMO–SUMO gaps are inherently narrower than the HOMO–LUMO gap of closed-shell molecules, enabling efficient NIR photothermal conversion.[26] Radicals **4a** (λ_{max} = 1113.2 nm, 5300 M^{-1} cm^{-1}) and **4b** (λ_{max} = 1330.7 nm, 4577 M^{-1} cm^{-1}) are among the few phosphorus-centered radicals exhibiting strong absorptions within the NIR-II biowindow.[37] Photothermal performance was evaluated using powdered samples in sealed NMR tubes monitored by an IR camera. Under 1064 nm laser irradiation at a powder density of 0.5 W cm^{-2}, compounds **4a** and **4b** exhibited a rapid temperature increases, reaching 63 °C and 56 °C within 180 s, respectively. In contrast, compounds **3a** (λ_{max} = 402.5 nm, 4251 M^{-1} cm^{-1}) and **3b** (λ_{max} = 569.1 nm, 753 M^{-1} cm^{-1}), along with blank controls, showed negligible heating (Fig. 6 and S24). After five consecutive irradiation cycles, both **4a** and **4b** powders showed negligible degradation in photothermal performance, demonstrating satisfactory thermal and photostability. This efficient photothermal conversion establishes **4a** and **4b** as the first phosphorus radical-based organic photothermal materials operating in the NIR-II region. Unfortunately, the high air sensitivity of these radicals limited their practical applications, necessitating the use of an inert atmosphere.

Conclusions

Building upon the 140 year legacy of the Büchner reaction,[1] this work demonstrates that aromatic biradicaloids undergo analogous Büchner-type ring expansions, as exemplified by the transformation of dicarbondiphosphides **1a,b** into aromatic 1,3-diphospholium cations **3a,b**. DFT calculations prove this process is kinetically accessible and thermodynamically favourable, proceeding through a classical [2 + 1] cycloaddition pathway. The 6π-aromaticity of **3a,b** is unequivocally supported by NMR, SC-XRD analysis, and quantum chemical calculations. Crucially, reduction of **3a,b** yields stable 7π-electron neutral radicals **4a,b**, which exhibit strong NIR-II absorption and efficient photothermal conversion. This study extends the scope of Büchner reaction to biradicaloid systems, and paves the way for

designing novel aromaticity-driven main-group transformations with potential applications in photothermal materials.

Author contributions

S. Liu carried out most of the experimental work. S. Zheng and J. Lin assisted with the NMR spectra and X-ray single crystallographic diffraction measurements. Z. Li carried out the computational studies. The manuscript was written through contributions of all authors. All authors have given approval to the final version of the manuscript.

Conflicts of interest

There are no conflicts to declare.

Data availability

CCDC 2464316–2464319 contain the supplementary crystallographic data for this paper.[38a–d]

All data associated with this article are available from SI. Supplementary information: Synthesis and characterization of compounds, NMR spectra, crystallographic, and computational details. See DOI: **https://doi.org/10.1039/d5sc06158j**.

Acknowledgements

This work was supported by the National Natural Science Foundation of China (22271315), Guangdong Basic and Applied Basic Research Foundation (2023A1515010092), National Key Research and Development Program of China (2021YFA1500401), Key Laboratory of Guangdong Higher Education Institutions of Northeast Guangdong New Functional Materials (2024KSYS021).

Notes and references

1 E. Buchner and T. Curtius, *Ber. Dtsch. Chem. Ges.*, 1885, **18**, 2371–2377.

2 (*a*) C.-Y. Shi, G.-Y. Zhu, Y. Xu, M.-Y. Teng and L.-W. Ye, *Chin. Chem. Lett.*, 2023, **34**, 108441; (*b*) S. E. Reisman, R. R. Nani and S. Levin, *Synlett*, 2011, **2011**, 2437–2442; (*c*) M. P. Doyle and D. C. Forbes, *Chem. Rev.*, 1998, **98**, 911–936; (*d*) T. Ye and M. A. McKervey, *Chem. Rev.*, 1994, **94**, 1091–1160; (*e*) A. J. Anciaux, A. Demonceau, A. F. Noels, A. J. Hubert, R. Warin and P. Teyssie, *J. Org. Chem.*, 1981, **46**, 873–876.

3 (*a*) M. Tamm, T. Bannenberg, R. Fröhlich, S. Grimme and M. Gerenkamp, *Dalton Trans.*, 2004, 482–491; (*b*) M. L. H. Green and D. K. P. Ng, *Chem. Rev.*, 1995, **95**, 439–473; (*c*) M. Tamm, B. Dreβel and R. Fröhlich, *J. Org. Chem.*, 2000, **65**, 6795–6797; (*d*) M. Tamm, T. Bannenberg, B. Dressel, R. Fröhlich and D. Kunz, *Organometallics*, 2001, **20**, 900–904.

4 (*a*) E. Ciganek, *J. Am. Chem. Soc.*, 1971, **93**, 2207–2215; (*b*) O. A. McNamara and A. R. Maguire, *Tetrahedron*, 2011, **67**, 9–40; (*c*) T. A. Perera, E. W. Reinheimer and T. W. Hudnall, *J. Am. Chem. Soc.*, 2017, **139**, 14807–14814.

5 (*a*) E. Ciganek, *J. Am. Chem. Soc.*, 1965, **87**, 652–653; (*b*) E. Ciganek, *J. Am. Chem. Soc.*, 1967, **89**, 1454–1458; (*c*) K. L. Smith, C. L. Padgett, W. D. Mackay and J. S. Johnson, *J. Am. Chem. Soc.*, 2020, **142**, 6449–6455.

6 (*a*) M. Kira, S. Ishida, T. Iwamoto and C. Kabuto, *J. Am. Chem. Soc.*, 2002, **124**, 3830–3831; (*b*) T. Kosai, S. Ishida and T. Iwamoto, *Angew. Chem., Int. Ed.*, 2016, **55**, 15554–15558; (*c*) T. Eisner, A. Kostenko, F. Hanusch and S. Inoue, *Chem.–Eur. J.*, 2022, **28**, e202202330; (*d*) D. Wendel, A. Porzelt, F. A. D. Herz, D. Sarkar, C. Jandl, S. Inoue and B. Rieger, *J. Am. Chem. Soc.*, 2017, **139**, 8134–8137; (*e*) H. Zhu, A. Kostenko, D. Franz, F. Hanusch and S. Inoue, *J. Am. Chem. Soc.*, 2023, **145**, 1011–1021.

7 (*a*) L. L. Liu, J. Zhou, L. L. Cao, R. Andrews, R. L. Falconer, C. A. Russell and D. W. Stephan, *J. Am. Chem. Soc.*, 2018, **140**, 147–150; (*b*) L. L. Liu, L. L. Cao, J. Zhou and D. W. Stephan, *Angew. Chem., Int. Ed.*, 2019, **58**, 273–277.

8 (*a*) J. Hicks, P. Vasko, J. M. Goicoechea and S. Aldridge, *J. Am. Chem. Soc.*, 2019, **141**, 11000–11003; (*b*) X. Zhang and L. L. Liu, *Angew. Chem., Int. Ed.*, 2022, **61**, e202116658; (*c*) X. Zhang and L. L. Liu, *Angew. Chem., Int. Ed.*, 2021, **60**, 27062–27069.

9 (*a*) L. Zhu, J. Zhang and C. Cui, *Inorg. Chem.*, 2019, **58**, 12007–12010; (*b*) H. Suzuki, N. Tokitoh and R. Okazaki, *J. Am. Chem. Soc.*, 1994, **116**, 11572–11573.

10 (*a*) Y. Chen, P. Su, D. Wang, Z. Ke and G. Tan, *Nat. Commun.*, 2024, **15**, 4579; (*b*) Q. Luo, T. Liu, L. Huang, C. Yang and W. Lu, *Angew. Chem., Int. Ed.*, 2024, **63**, e202405122; (*c*) L. L. Liu, J. Zhou, R. Andrews and D. W. Stephan, *J. Am. Chem. Soc.*, 2018, **140**, 7466–7470; (*d*) T. G. Saint-Denis, T. A. Wheeler, Q. Chen, G. Balázs, N. S. Settineri, M. Scheer and T. D. Tilley, *J. Am. Chem. Soc.*, 2024, **146**, 4369–4374.

11 (*a*) A. Mizuno, R. Matsuoka, T. Mibu and T. Kusamoto, *Chem. Rev.*, 2024, **124**, 1034–1121; (*b*) J. A. Meckes, Z. W. Schroeder, D. Sarkar, R. W. Hooper, C. E. Faraday-Smith, A. Brown, R. R. Tykwinski and V. K. Michaelis, *J. Am. Chem. Soc.*, 2025, **147**, 7293–7304; (*c*) A. Mizuno, R. Matsuoka, S. Kimura, K. Ochiai and T. Kusamoto, *J. Am. Chem. Soc.*, 2024, **146**, 18470–18483; (*d*) R. Casares, S. Rodríguez-González, Á. Martínez-Pinel, I. R. Márquez, M. T. González, C. Díaz, F. Martín, J. M. Cuerva, E. Leary and A. Millán, *J. Am. Chem. Soc.*, 2024, **146**, 29977–29986; (*e*) Z. Zhu, D. Zhang, T. Xiao, Y.-H. Fang, X. Xiao, X.-G. Wang, S.-D. Jiang and D. Zhao, *Angew. Chem., Int. Ed.*, 2023, **62**, e202314900; (*f*) C. Shu, Z. Yang and A. Rajca, *Chem. Rev.*, 2023, **123**, 11954–12003; (*g*) Y. Ishigaki, T. Harimoto, T. Shimajiri and T. Suzuki, *Chem. Rev.*, 2023, **123**, 13952–13965; (*h*) Q. Liu, K. Onishi, Y. Miyazawa, Z. Wang, S. Hatano and M. Abe, *J. Am. Chem. Soc.*, 2023, **145**, 27089–27094; (*i*) Y. Zhao, Y. Zhang, T. Wang, R. Pei, Y. Zhao, X.-S. Xue and X. Wang, *Angew. Chem., Int. Ed.*, 2024, **63**, e202411180; (*j*) J. Wang, H. Cui, H. Ruan, Y. Zhao, Y. Zhao, L. Zhang and X. Wang, *J. Am. Chem. Soc.*, 2022, **144**, 7978–7982; (*k*) Z. Feng, Y. Chong, S. Tang,

Y. Fang, Y. Zhao, J. Jiang and X. Wang, *Chem. Sci.*, 2021, **12**, 15151–15156; (*l*) H. Cui, Z.-B. Hu, C. Chen, H. Ruan, Y. Fang, L. Zhang, Y. Zhao, G. Tan, Y. Song and X. Wang, *Chem. Sci.*, 2021, **12**, 9998–10004; (*m*) W. Yang, L. Zhang, D. Xiao, R. Feng, W. Wang, S. Pan, Y. Zhao, L. Zhao, G. Frenking and X. Wang, *Nat. Commun.*, 2020, **11**, 3441; (*n*) S. Tang, L. Zhang, H. Ruan, Y. Zhao and X. Wang, *J. Am. Chem. Soc.*, 2020, **142**, 7340–7344; (*o*) C. Chen, H. Ruan, Z. Feng, Y. Fang, S. Tang, Y. Zhao, G. Tan, Y. Su and X. Wang, *Angew. Chem., Int. Ed.*, 2020, **59**, 11794–11799; (*p*) H. Han, D. Zhang, Z. Zhu, R. Wei, X. Xiao, X. Wang, Y. Liu, Y. Ma and D. Zhao, *J. Am. Chem. Soc.*, 2021, **143**, 17690–17700; (*q*) Y. Pilopp, H. Beer, J. Bresien, D. Michalik, A. Villinger and A. Schulz, *Chem. Sci.*, 2025, **16**, 876–888; (*r*) T. Jiao, C.-H. Wu, Y.-S. Zhang, X. Miao, S. Wu, S.-D. Jiang and J. Wu, *Nat. Chem.*, 2025, **17**, 924–932.

12 (*a*) M. Abe, *Chem. Rev.*, 2013, **113**, 7011–7088; (*b*) J. A. Berson, *Science*, 1994, **266**, 1338–1339; (*c*) A. Rajca, *Chem. Rev.*, 1994, **94**, 871–893.

13 (*a*) Z. Feng, S. Tang, Y. Su and X. Wang, *Chem. Soc. Rev.*, 2022, **51**, 5930–5973; (*b*) K. Ota and R. Kinjo, *Chem. Soc. Rev.*, 2021, **50**, 10594–10673; (*c*) N. M. Gallagher, J. J. Bauer, M. Pink, S. Rajca and A. Rajca, *J. Am. Chem. Soc.*, 2016, **138**, 9377–9380; (*d*) E. Zander, J. Bresien, V. V. Zhivonitko, J. Fessler, A. Villinger, D. Michalik and A. Schulz, *J. Am. Chem. Soc.*, 2023, **145**, 14484–14497; (*e*) J. Bresien, A. Schulz, L. S. Szych, A. Villinger and R. Wustrack, *Dalton Trans.*, 2019, **48**, 11103–11111; (*f*) K. Takeuchi, M. Ichinohe and A. Sekiguchi, *J. Am. Chem. Soc.*, 2011, **133**, 12478–12481; (*g*) X. Wang, Y. Peng, M. M. Olmstead, J. C. Fettinger and P. P. Power, *J. Am. Chem. Soc.*, 2009, **131**, 14164–14165; (*h*) C. Cui, M. Brynda, M. M. Olmstead and P. P. Power, *J. Am. Chem. Soc.*, 2004, **126**, 6510–6511; (*i*) H. Cox, P. B. Hitchcock, M. F. Lappert and L. J.-M. Pierssens, *Angew. Chem., Int. Ed.*, 2004, **43**, 4500–4504.

14 (*a*) T. Beweries, R. Kuzora, U. Rosenthal, A. Schulz and A. Villinger, *Angew. Chem., Int. Ed.*, 2011, **50**, 8974–8978; (*b*) E. Niecke, A. Fuchs, F. Baumeister, M. Nieger and W. W. Schoeller, *Angew. Chem., Int. Ed. Engl.*, 1995, **34**, 555–557.

15 (*a*) A. Hinz, A. Schulz and A. Villinger, *J. Am. Chem. Soc.*, 2015, **137**, 9953–9962; (*b*) A. Hinz, A. Schulz and A. Villinger, *Chem. Sci.*, 2016, **7**, 745–751; (*c*) A. Hinz, A. Schulz and A. Villinger, *Angew. Chem., Int. Ed.*, 2015, **54**, 2776–2779.

16 (*a*) C. Saalfrank, F. Fantuzzi, T. Kupfer, B. Ritschel, K. Hammond, I. Krummenacher, R. Bertermann, R. Wirthensohn, M. Finze, P. Schmid, V. Engel, B. Engels and H. Braunschweig, *Angew. Chem., Int. Ed.*, 2020, **59**, 19338–19343; (*b*) M. K. Sharma, F. Ebeler, T. Glodde, B. Neumann, H.-G. Stammler and R. S. Ghadwal, *J. Am. Chem. Soc.*, 2021, **143**, 121–125; (*c*) T. Sugahara, J.-D. Guo, D. Hashizume, T. Sasamori and N. Tokitoh, *J. Am. Chem. Soc.*, 2019, **141**, 2263–2267; (*d*) M. K. Sharma, D. Rottschäfer, T. Glodde, B. Neumann, H.-G. Stammler and R. S. Ghadwal, *Angew. Chem., Int. Ed.*, 2021, **60**, 6414–6418.

17 (*a*) A. Schulz, *Dalton Trans.*, 2018, **47**, 12827–12837; (*b*) L. Chojetzki, A. Schulz, A. Villinger and R. Wustrack, *Z. Anorg. Allg. Chem.*, 2020, **646**, 614–624; (*c*) H. Beer, A. Linke, J. Bresien, A. Villinger and A. Schulz, *Inorg. Chem. Front.*, 2022, **9**, 2659–2667; (*d*) J. Rosenboom, L. Chojetzki, T. Suhrbier, J. Rabeah, A. Villinger, R. Wustrack, J. Bresien and A. Schulz, *Chem.–Eur. J.*, 2022, **28**, e202200624; (*e*) Z. Li, Y. Hou, Y. Li, A. Hinz and X. Chen, *Chem.–Eur. J.*, 2018, **24**, 4849–4855; (*f*) X. Chen, L. L. Liu, S. Liu, H. Grützmacher and Z. Li, *Angew. Chem., Int. Ed.*, 2020, **59**, 23830–23835; (*g*) S. Liu, Y. Li, J. Lin, Z. Ke, H. Grützmacher, C.-Y. Su and Z. Li, *Chem. Sci.*, 2024, **15**, 5376–5384; (*h*) J. Rosenboom, A. Villinger, A. Schulz and J. Bresien, *Dalton Trans.*, 2022, **51**, 13479–13487; (*i*) A. Hinz, R. Kuzora, U. Rosenthal, A. Schulz and A. Villinger, *Chem.–Eur. J.*, 2014, **20**, 14659–14673; (*j*) F. Ebeler, B. Neumann, H.-G. Stammler, I. Fernández and R. S. Ghadwal, *J. Am. Chem. Soc.*, 2024, **146**, 34979–34989.

18 (*a*) Z. Li, X. Chen, D. M. Andrada, G. Frenking, Z. Benkö, Y. Li, J. R. Harmer, C.-Y. Su and H. Grützmacher, *Angew. Chem., Int. Ed.*, 2017, **56**, 5744–5749; (*b*) D. Rottschäfer, B. Neumann, H.-G. Stammler and R. S. Ghadwal, *Chem.–Eur. J.*, 2017, **23**, 9044–9047.

19 (*a*) Z. Li, X. Chen, L. L. Liu, M. T. Scharnhölz and H. Grützmacher, *Angew. Chem., Int. Ed.*, 2020, **59**, 4288–4293; (*b*) M. T. Scharnhölz, P. Coburger, L. Gravogl, D. Klose, J. J. Gamboa-Carballo, G. Le Corre, J. Bösken, C. Schweinzer, D. Thöny, Z. Li, K. Meyer and H. Grützmacher, *Angew. Chem., Int. Ed.*, 2022, **61**, e202205371; (*c*) P. Coburger, F. Masero, J. Bösken, V. Mougel and H. Grützmacher, *Angew. Chem., Int. Ed.*, 2022, **61**, e202211749.

20 D. Zuber, S. Frei and P. Coburger, *ChemistryEurope*, 2025, e202500199.

21 P. Coburger, D. Zuber, C. Schweinzer and M. Scharnhölz, *Chem.–Eur. J.*, 2024, **30**, e202302970.

22 P. L. Floch, *Coord. Chem. Rev.*, 2006, **250**, 627–681.

23 (*a*) P. Bellotti, M. Koy, M. N. Hopkinson and F. Glorius, *Nat. Rev. Chem.*, 2021, **5**, 711–725; (*b*) A. Doddi, M. Peters and M. Tamm, *Chem. Rev.*, 2019, **119**, 6994–7112; (*c*) M. N. Hopkinson, C. Richter, M. Schedler and F. Glorius, *Nature*, 2014, **510**, 485–496.

24 (*a*) Y. Schulte, C. Wölper, S. M. Rupf, M. Malischewski, D. J. SantaLucia, F. Neese, G. Haberhauer and S. Schulz, *Nat. Chem.*, 2024, **16**, 651–657; (*b*) D. Shi, X. Tian, S. Wu, Y. Huang, J. Xu, Z. Zhai, L. Xie, Y. Li and Z. Sun, *Chin. J. Chem.*, 2025, **43**, 531–535; (*c*) Y. Schulte, B. L. Geoghegan, C. Helling, C. Wölper, G. Haberhauer, G. E. Cutsail, III and S. Schulz, *J. Am. Chem. Soc.*, 2021, **143**, 12658–12664; (*d*) W. Yang, K. E. Krantz, L. A. Freeman, D. A. Dickie, A. Molino, G. Frenking, S. Pan, D. J. D. Wilson and R. J. Gilliard Jr., *Angew. Chem., Int. Ed.*, 2020, **59**, 3850–3854; (*e*) Y. Tian, K. Uchida, H. Kurata, Y. Hirao, T. Nishiuchi and T. Kubo, *J. Am. Chem. Soc.*, 2014, **136**, 12784–12793; (*f*) T. Kitagawa, K. Ogawa and K. Komatsu, *J. Am. Chem. Soc.*, 2004, **126**, 9930–9931; (*g*) H. Sitzmann and R. Boese, *Angew. Chem., Int. Ed. Engl.*, 1991, **30**, 971–973.

25 (*a*) A. M. Smith, M. C. Mancini and S. Nie, *Nat. Nanotechnol.*, 2009, **4**, 710–711; (*b*) H. Lin, S. Gao, C. Dai, Y. Chen and J. Shi, *J. Am. Chem. Soc.*, 2017, **139**, 16235–16247.

26 (*a*) Q. Zhao, C. Wu, Y. Gao, J. Long, W. Zhang, Y. Chen, Y. Yang, Y. Luo, Y. Lai, H. Zhang, X. Chen, F. Li and S. Li, *Advanced Science*, 2025, **12**, 2411733; (*b*) J. Zhang, H. Luo, W. Ma, J. Lv, B. Wang, F. Sun, W. Chi, Z. Fang and Z. Yang, *Advanced Science*, 2025, **12**, 2500293; (*c*) X. Tian, M. Wang, L. Ye, Y. Gao, G. Yu, M. Lv, X. Ma, L. Ma and Z. Sun, *Precis. Chem.*, 2025, **3**, 389–398; (*d*) B. Tang, W.-L. Li, Y. Chang, B. Yuan, Y. Wu, M.-T. Zhang, J.-F. Xu, J. Li and X. Zhang, *Angew. Chem., Int. Ed.*, 2019, **58**, 15526–15531; (*e*) S. Kong, L. Yang, Q. Sun, T. Wang, R. Pei, Y. Zhao, W. Wang, Y. Zhao, H. Cui, X. Gu and X. Wang, *Angew. Chem., Int. Ed.*, 2024, **63**, e202400913.

27 X. Zhang, X. Chen, H. Zhai, S. Liu, C. Hu, L. L. Liu, S. Wang and Z. Li, *Dalton Trans.*, 2020, **49**, 6384–6390.

28 X. Chen, C. Hu, X. Zhang, S. Liu, Y. Mei, G. Hu, L. L. Liu, Z. Li and C.-Y. Su, *Inorg. Chem.*, 2021, **60**, 5771–5778.

29 (*a*) P. Pyykkö and M. Atsumi, *Chem.–Eur. J.*, 2009, **15**, 12770–12779; (*b*) F. H. Allen, O. Kennard, D. G. Watson, L. Brammer, A. G. Orpen and R. Taylor, *J. Chem. Soc. Perkin Trans. 2*, 1987, S1–S19.

30 (*a*) C. C. Chong, B. Rao, R. Ganguly, Y. Li and R. Kinjo, *Inorg. Chem.*, 2017, **56**, 8608–8614; (*b*) R. Yadav, A. Sharma, B. Das, C. Majumder, A. Das, S. Sen and S. Kundu, *Chem.–Eur. J.*, 2024, **30**, e202401730.

31 M. J. Frisch and *et al.*, *Gaussian 16, Revision C.01*, 2016.

32 G. Knizia and J. E. M. N. Klein, *Angew. Chem., Int. Ed.*, 2015, **54**, 5518–5522.

33 A. Bondi, *J. Phys. Chem.*, 1964, **68**, 441–451.

34 Y. Pilopp, J. Bresien, K. P. Lüdtke and A. Schulz, *Chem.–Eur. J.*, 2025, **31**, e202403893.

35 C. Xu and K. Pu, *Chem. Soc. Rev.*, 2021, **50**, 1111–1137.

36 (*a*) J.-C. Liu, T. Li, H. Yu, J. Y. Huang, P.-X. Li, Z.-Y. Ruan, P.-Y. Liao, C. Ou, Y. Feng and M.-L. Tong, *Angew. Chem., Int. Ed.*, 2025, **64**, e202413805; (*b*) T. Li, J.-C. Liu, E.-P. Liu, B.-T. Liu, J.-Y. Wang, P.-Y. Liao, J.-H. Jia, Y. Feng and M.-L. Tong, *Chem. Sci.*, 2024, **15**, 1692–1699; (*c*) N. Yang, S. Song, C. Liu, J. Ren, X. Wang, S. Zhu and C. Yu, *Biomater. Sci.*, 2022, **10**, 4815–4821; (*d*) Y. Chen, H. Yu, Y. Wang, P. Sun, Q. Fan and M. Ji, *Biomater. Sci.*, 2022, **10**, 2772–2788.

37 (*a*) B. Das, A. Makol and S. Kundu, *Dalton Trans.*, 2022, **51**, 12404–12426; (*b*) Y. H. Budnikova, *Dokl. Chem.*, 2022, **507**, 229–259.

38 (*a*) S. Liu S. Zheng J. Lin H. Grützmacher C.-Y. Su and Z. Li, CCDC 2464316: Experimental Crystal Structure Determination, 2025, DOI: **10.5517/ccdc.csd.cc2nqb2t**; (*b*) S. Liu S. Zheng J. Lin H. Grützmacher C.-Y. Su and Z. Li, CCDC 2464317: Experimental Crystal Structure Determination, 2025, DOI: **10.5517/ccdc.csd.cc2nqb3v**; (*c*) S. Liu S. Zheng J. Lin H. Grützmacher C.-Y. Su and Z. Li, CCDC 2464318: Experimental Crystal Structure Determination, 2025, DOI: **10.5517/ccdc.csd.cc2nqb4w**; (*d*) S. Liu S. Zheng J. Lin H. Grützmacher C.-Y. Su and Z. Li, CCDC 2464319: Experimental Crystal Structure Determination, 2025, DOI: **10.5517/ccdc.csd.cc2nqb5x**.